Smart Materials and Structures



# Size-dependent thermo-electrical buckling analysis of functionally graded piezoelectric nanobeams

**IOP** Publishing Smart Materials and Structures

Smart Mater. Struct. **24** (2015) 125007 (17pp) doi:10.1088/0964-1726/24/12/125007

# Size-dependent thermo-electrical buckling analysis of functionally graded piezoelectric nanobeams

**Farzad Ebrahimi and Erfan Salari**

Department of Mechanical Engineering, Faculty of Engineering, Imam Khomeini International University, Qazvin, Iran

E-mail: febrahimy@eng.ikiu.ac.ir

Received 8 July 2015, revised 3 September 2015
Accepted for publication 28 September 2015
Published 27 October 2015

**Abstract**

In the present study, thermo-electrical buckling characteristics of functionally graded piezoelectric (FGP) Timoshenko nanobeams subjected to in-plane thermal loads and applied electric voltage are carried out by presenting a Navier type solution for the first time. Three kinds of thermal loading, namely, uniform, linear and nonlinear temperature rises through the thickness direction are considered. Thermo-electro-mechanical properties of FGP nanobeam are supposed to vary smoothly and continuously throughout the thickness based on power-law model. Eringen's nonlocal elasticity theory is exploited to describe the size dependency of nanobeam. Using Hamilton's principle, the nonlocal governing equations together with corresponding boundary conditions based on Timoshenko beam theory are obtained for the thermal buckling analysis of graded piezoelectric nanobeams including size effect and they are solved applying analytical solution. According to the numerical results, it is revealed that the proposed modeling can provide accurate critical buckling temperature results of the FG nanobeams as compared some cases in the literature. In following a parametric study is accompanied to examine the effects of the several parameters such as various temperature distributions, external electric voltage, power-law index, nonlocal parameter and aspect ratio on the critical buckling temperature difference of the size-dependent FGP nanobeams in detail. It is found that the small scale effect and electrical loading have a significant effect on buckling temperatures of FGP nanobeams.

Keywords: functionally graded piezoelectric nanobeam, nonlocal elasticity theory, size effect

(Some figures may appear in colour only in the online journal)

## 1. Introduction

The piezoelectric materials stand as a class of smart structures which are widely used as sensors and actuators in control systems due to their excellent electromechanical properties, easy fabrication, design flexibility, and efficiency to convert electrical energy into mechanical energy. The ability of piezoelectric materials to surpass the vibrational motion, shape control, and delay the buckling have necessitated more investigations on the behavior of structures including piezoelectricity effects (Ebrahimi and Rastgo 2008). However, because of the superior properties of these smart materials, piezoelectric nanostructures have been regarded as the next-generation piezoelectric materials because of their inherent nanosized piezoelectricity. These distinct features make them suitable for potential applications in micro electro-mechanical systems (MEMS) and nano electro-mechanical systems (NEMS) such as nanogenerators (Wang and Song 2006), field effect transistors (Fei *et al* 2009), piezoelectric gated diodes (He *et al* 2007), gas sensors (Wan *et al* 2004), nanowire resonators and oscillators (Tanner *et al* 2007).

Functionally graded materials (FGMs), a novel generation of composites of microscopical heterogeneity initiated by a group of Japanese scientists in the mid-1980s, are achieved by controlling the volume fractions, microstructure, porosity, etc of the material constituents during manufacturing, resulting in spatial gradient of macroscopic material properties of mechanical strength and thermal conductivity. In comparison with traditional composites, FGMs possess various advantages, for instance, ensuring smooth transition of stress distributions, minimization or elimination of stress concentration, and increased bonding strength along the interface of two dissimilar materials. In the last decade, beams and plates made of FGMs have found wide applications as structural elements in modern industries such as aeronautics/astronautics manufacturing industry, mechanical engineering and engine combustion chamber, nuclear engineering and reactors. Motivated by these engineering applications, ceramic-metal FGMs have also attracted intensive research interests, which were mainly focused on their static, dynamic and buckling characteristics of FG structures (Ebrahimi *et al* 2009).

Moreover, nanoscale engineering materials have attracted great interest in modern science and technology after the invention of carbon nanotubes (CNTs) by Iijima (1991). They have significant mechanical, thermal and electrical performances that are superior to the conventional structural materials. Beam elements are one of the basic components in micro/nano electromechanical systems, biomedical sensors, actuators, transistors, probes, and resonators. In these nanodevices, the dimension may vary from several hundred nanometers to just a few nanometers. Therefore, understanding the mechanical and physical behaviors of the nanobeams made of piezoelectric materials or those incorporated with piezoelectric layer is of necessary in the design of the nanodevices.

The classical continuum theory is quite efficient in the mechanical analysis of the macroscopic structures, but its applicability to the identification of the size effect on the mechanical behaviors on micro- or nano-scale structures is questionable. This limitation of the classical continuum theory is partly due to the fact that the classical continuum theory does not admit the size dependence in the elastic solutions of inclusions and inhomogeneities. However the classical continuum models need to be extended to consider the nanoscale effects and this can be achieved through the nonlocal elasticity theory proposed by Eringen (2002) which consider the size-dependent effect. According to this theory, the stress state at a reference point is considered as a function of strain states of all points in the body. This nonlocal theory is proved to be in accordance with atomic model of lattice dynamics and with experimental observations on phonon dispersion (Eringen 1983). In the field of nonlocal elasticity theory, Pradhan and Mandal (2013) investigated the thermal vibration, buckling and bending characteristics of CNTs by using finite element method (FEM) based on Timoshenko beam theory. Ke *et al* (2012) and Ke and Wang (2012) studied the free vibration analysis of the piezoelectric Timoshenko nanobeams under thermo-electro-mechanical field based on the Eringen's theory. They noticed that the values of uniform temperature change, nonlocal parameter and applied voltage play a significant role in the vibrational response of the piezoelectric nanobeams.

Nowadays, with the development in nanotechnology, FGMs have also been employed in MEMS/NEMS (Witvrouw and Mehta 2005, Lee *et al* 2006). Actually, FGMs find increasing applications in micro- and nano-scale structures such as thin films in the form of shape memory alloys (Fu *et al* 2003, Lü *et al* 2009), atomic force microscopes (AFMs) (Rahaeifard *et al* 2009), micro sensors, micro piezoactuator and nano-motors (Lun *et al* 2006, Carbonari *et al* 2009). In all of these applications, the size effect plays major role which should be considered to study the mechanical behaviors of such small scale structures. Beams are the core structures widely used in MEMS, NEMS and AFMS with the order of microns or sub-microns, and their properties are closely related to their microstructures. On the other hands, FG nanobeams are important structural elements and hence, because of high sensitivity of MEMS/NEMS to external stimulations, understanding mechanical properties and thermal buckling behavior of them are of significant importance to the design and manufacture of FG MEMS/NEMS. Furthermore, different fabrication processes of nanoscale FGM have been focused by the several researchers (Kim *et al* 2009, Kerman *et al* 2012). Also, FG nanobeams are innovative nanocomposite materials that are designed to have a smooth variation of material properties across particular dimensions. This can be attained by fabricating the nanocomposite material to have a gradually spatial variation of the relative volume fractions as well as microstructure of its constitutive materials. Actually, the choice of material phases is affected by functional performance necessities. For instant, in a nanoscale metal/ceramic FGM structure, the metal-rich side is typically located in regions, where the toughness should to be high. In contrast, the ceramic-rich side is commonly placed in regions with high temperature gradients. The expected advantages of miniaturized FGMs to nanocomposites are: magnification the interface bond strength through introducing a continuous gradation of composition, elimination of deleterious stress concentrations at the intersection of interfaces, reduction of the peak thermal stresses, and enhancement fracture toughness of brittle ceramics by implementing a metallic phase. Therefore, establishing an accurate model of FG nanobeams is a key issue for successful NEMS design.

Based on the above discussions, thermal buckling and free vibration characteristics of FGM structures have also been of interest of many investigators. Among them, Nateghi and Salamat-talab (2013) investigated thermal effect on buckling and free vibration behavior of temperature-independent FG microbeams based on modified couple stress theory and using generalized differential quadrature (DQ) method. They showed that higher temperature changes signify size dependency of FG microbeam. The free vibration analysis of FG beams via several axiomatic refined theories was presented by Giunta *et al* (2011) based on Navier type solution. They assumed that the material properties of FG beam graded in the thickness direction according to the power law distribution. It was found that the efficiency of the proposed models is good since the computational time is less than a second for the highest considered approximation order, whereas for the three-dimensional FEM solution it can be three order of magnitude higher. In another study, thermo-mechanical behavior of functionally graded beams based on several beam models was proposed by Giunta *et al* (2013). It has been shown that the considered thermomechanical problems, although presenting a global bending deformation, are governed by three-dimensional stress fields that call for very accurate models. Employing modified couple stress theory the thermo-mechanical buckling behavior of FG microbeams embedded in elastic medium based on sinusoidal beam theory was presented by Akgöz and Civalek (2014). It is found that the size-dependency on buckling analysis of FG microbeam is more considerable for lower values of length scale parameter. Eltaher *et al* (2013) applied a finite element formulation for static-buckling analysis of FG nanobeams based on nonlocal Euler beam theory. Also, Kiani and Eslami (2010) in their study investigated thermally induced instability of Euler–Bernoulli FGM beams with various boundary conditions. In this study, they observed that the buckling temperature of FGM beam depends upon the modulus of elasticity of steel and ceramic constituents. Mashat *et al* (2014) utilized Carrera unified formulation to model the free vibration analysis of FG structures within the framework of the FEM. They concluded that the implementation of the finite elements in accordance with the Carrera unified formulation made it possible to consider a great variety of structures and boundary conditions. Also, Fallah and Aghdam (2012) used Euler–Bernoulli beam theory to investigate thermos-mechanical buckling and nonlinear vibration analysis of functionally graded beams on nonlinear elastic foundation. Additionally, using nonlocal Timoshenko and Euler–Bernoulli beam theory, Şimşek and Yurtcu (2013) investigated bending and buckling of FG nanobeam by analytical method. Recently, Niknam and Aghdam (2015) have performed a semi analytical approach for large amplitude free vibration and buckling of FG nanobeams resting on elastic foundation based on nonlocal elasticity theory. They discussed that the effect of small scale parameter decreases by increasing length of the beam. More recently, Ebrahimi and Salari (2015a) studied thermal effects on free vibration of functionally graded nanobeam within the framework of Euler–Bernoulli beam model on the basis of nonlocal elasticity theory. They developed their previous works by analyzing thermal buckling and free vibration behavior of FG nanobeams based on the Timoshenko beam theory, too (Ebrahimi and Salari 2015b). It should be noted that the above mentioned studies dealt with the micro and nanobeams made of ceramic-metal FGMs because of their high mechanical–thermal resistant.

Moreover, conventional piezoelectric sensors and actuators are often made of several layers of different piezoelectric materials. The principal weakness of these types of structures is that the high stress concentrations are usually appeared at the interlayer surfaces under mechanical or electrical loading. This drawback reduces the electrical field induced displacement characteristics, lifetime, integrity and reliability of piezoelectric devices, and also restricts the usefulness of piezoelectric actuators in the area of measured devices requiring high reliability. In order to overcome the aforementioned disadvantages of the traditional layered piezoelectric structures, a novel class of piezoelectric materials called functionally graded piezoelectric materials (FGPMs) has been presented and fabricated by using the metallurgical science and powder mold stacking press technique in which mechanical and electrical properties change continuously in one or more directions (Zhu and Meng 1995).

Finally, reported papers on FGPMs subjected to thermo-electro-mechanical loads are limited in number. For instance, by using DQ method, the static bending, free vibration and dynamic analysis of monomorph, bimorph, and multimorph FGPM beams under the action of thermal, mechanical, and electrical loadings were presented by Yang and Xiang (2007) based on the Timoshenko beam theory. They assumed that the material properties of FGP beam graded in the thickness direction according to the power-law model. A closed form solution for the FGPM cantilever beams subjected to different loadings and based on the two dimensional theory of elasticity and the Airy stress function was proposed by Shi and Chen (2004). Additionally, based on the linear piezoelectricity theory, Zhong and Yu (2007) discussed a general solution on the electrostatic analysis of an FGP beam under various boundary conditions with arbitrary graded material properties along the beam thickness direction. Kiani *et al* (2011) proposed the critical buckling temperature of Timoshenko FGM beams with surface-bonded piezoelectric layers subjected to both thermal loading and constant electric voltage. It was shown that increasing the thickness of piezoelectric FGM beam, the critical buckling temperature difference increases. Doroushi *et al* (2011) used higher order shear deformation of Reddy beam theory to investigate thermo-electro-mechanical free and forced vibration analysis of FGPM beams. They solved their problem by using FE method. In another study, Komijani *et al* (2013) analyzed nonlinear free vibration and post-buckling analysis of piezoelectric beams with graded properties based on Timoshenko beam theory. They showed that due to the non-symmetric distribution of material properties in the thickness direction, the linear critical buckling may not take place in this type of graded beams. Xiang and Shi (2009) predicted bending analysis of FGP sandwich cantilever under an applied electric field and heat conduction thermal load based on Airy stress function method. Also, thermo-mechanical geometrically nonlinear static and dynamic analysis of FG beams integrated with a pair of sensor layers made of FGP materials were studied by Bodaghi *et al* (2014). They concluded that the gradient indexes of FGP have a noticeable effect on their output voltages. Lezgy-Nazargah *et al* (2013) recommended an efficient three nodded finite element model for static, free vibration and dynamic response of FGPM beams. Recently, Komijani *et al* (2014) utilized modified couple stress theory to model the nonlinear deflection response of a monomorph microstructure-dependent FGPM beams based on Timoshenko beam theory. They also observed that the value of length scale parameter and the type of imposed load has significant effect on the nonlinear deflection behavior of FGPM beams.

To the authors' best knowledge, there is no work reported in the literature on the effects of various thermal environment and nanostructure dependency on the thermo-electrical buckling response of functionally graded piezoelectric nanobeams based on nonlocal elasticity theory. The common use of FGPM beams in high temperature environment leads to considerable changes in material properties.

These structures are often subjected to severe thermal environments during manufacturing and working, and thus the thermal effects become a primary design factor in specific cases. It is well known that the temperature rise leads to the reduction in the stiffness of the beams due to softening of the materials as well as the development of thermal stresses due to the thermal expansion. These effects in turn cause a quite significant change in the static and dynamic behaviors of the nanobeams. Consequently, thermal effects become important when the FGP nanodevice has to operate in either extremely hot or cold temperature environments. Therefore, there is strong scientific need to understand the thermal buckling behavior of graded piezoelectric nanobeams under thermal and electrical loadings. According to this fact, in this study, thermal buckling characteristics of FGP nanobeams considering the effect of three types of thermal loads namely, uniform, linear and nonlinear temperature rises (NLTRs) across the thickness is analyzed. An analytical method called Navier solution is employed for thermo-electrical buckling analysis of FG piezoelectric nanobeams for the first time. The thermo-electro-mechanical material properties of the beam is assumed to be graded in the thickness direction according to the power law distribution. Timoshenko beam theory, incorporated with Eringen's nonlocal elasticity theory, is employed to derive the nonlocal governing equations. The Hamilton's principle is used to achieve to the governing equations and boundary conditions for the thermal buckling of a nonlocal FGP nanobeam. These equations are solved using Navier type method and numerical solutions are obtained. The detailed mathematical derivations are presented while the emphasis is placed on investigating the effect of several parameters such as external electric voltage, different temperature distributions, power-law index and length scale parameter on buckling characteristics of size-dependent FGP nanobeams. Comparison between results of the present study and those available data in literature shows the accuracy of this model. Due to lack of similar results on the thermo-electrical response of FGP nanostructure, this study is likely to fill a gap in the state of the art of this problem.

## 2. Theoretical formulations

### 2.1. The material properties of FGP nanobeams

Consider a FGP nanobeam made of PZT-4 and PZT-5H piezoelectric materials with length $L$ in $x$ direction and uniform thickness $h$ in $z$ direction, and subjected to an electric potential $\Phi(x, z, t)$, as shown in figure 1. The effective material properties of the FGPM beam are assumed to vary continuously in the thickness direction ($z$-axis direction)

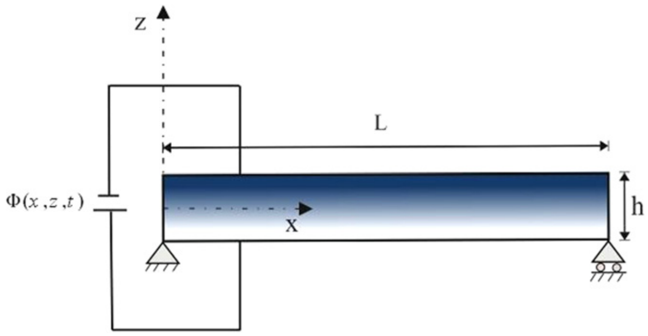


**Figure 1.** Schematic configuration of a functionally graded piezoelectric nanobeam.

according to a power function of the volume fractions of the constituents. Based on the power-law model, the effective material properties, $P$, can be considered as below (Komijani *et al* 2014):

$$P = P_u V_u + P_l V_l, \tag{1}$$

where $(P_l, P_u)$ are the material properties at the lower and upper surfaces, respectively, and $(V_l, V_u)$ are the corresponding volume fractions related by:

$$V_u = \left(\frac{z}{h} + \frac{1}{2}\right)^p, \quad V_l = 1 - V_u. \tag{2}$$

Therefore, from equations (1) and (2), the effective thermo-electro-mechanical material properties of the FGP beam can be expressed as:

$$P(z) = \left(P_u - P_l\right)\left(\frac{z}{h} + \frac{1}{2}\right)^p + P_l \tag{3}$$

here $p$ is the non-negative power-law exponent which determines the material distribution through the thickness of the beam and $z$ is the distance from the mid-plane of the graded piezoelectric beam. According to this distribution, the top surface ($z = h/2$) of FGP nanobeam is PZT-4 rich, whereas the bottom surface ($z = -h/2$) is PZT-5H rich.

### 2.2. Nonlocal elasticity theory for the piezoelectric materials

Based on the concept of nonlocal elasticity, stress at a point of continuum body depends on strain at all neighbor points. But, for FG materials, Eringen's nonlocal constitutive equations incorporate material properties and elasticity modulus, of neighbor points in the definition of nonlocal stress. Hence, the nonlocal theory should be modified by removing the effects of material properties at neighbor points from nonlocal constitutive equations. It should be pointed out that the material properties of FG nanobeam are only functions of thickness coordinate $z$, thus for the present problem, the modified nonlocal theory is converted to Eringen's nonlocal theory, similar to the assumption considered in (Niknam and Aghdam 2015, Salehipour *et al* 2015).

Unlike the constitutive equation in classical elasticity, Eringen's nonlocal theory (Eringen 1983, 2002) states that the stress at a reference point $x$ in a body is considered as a function of strains of all points $x'$ in the near region. This assumption is agreement with experimental observations of atomic theory and lattice dynamics in phonon scattering in which for a nonlocal piezoelectric solid the basic equations with zero body force may be obtained as (Ke *et al* 2012):

$$\sigma_{ij} = \int_V \alpha(|x' - x|, \tau)\big[C_{ijkl}\varepsilon_{kl}(x') - e_{kij}E_k(x') - C_{ijkl}\alpha_{kl}\Delta T\big]\mathrm{d}V(x') \tag{4a}$$

$$D_i = \int_V \alpha(|x' - x|, \tau)\big[e_{ikl}\varepsilon_{kl}(x') + k_{ik}E_k(x') + p_i\Delta T\big]\mathrm{d}V(x') \tag{4b}$$

in which $\sigma_{ij}$, $\varepsilon_{ij}$, $D_i$ and $E_i$ are the stress, strain, electric displacement and electric field components, respectively; $\alpha_{kl}$ and $\Delta T$ are the thermal expansion coefficient and temperature change, respectively; $C_{ijkl}$, $e_{kij}$, $k_{ik}$ and $p_i$ are elastic, piezoelectric, dielectric and pyroelectric constants, respectively; $\alpha(|x' - x|, \tau)$ is the nonlocal kernel function and $|x' - x|$ is the Euclidean distance. $\tau = e_0 a/l$ is defined as scale coefficient, where $e_0$ is a material constant which is determined experimentally or approximated by matching the dispersion curves of plane waves with those of atomic lattice dynamics; and $a$ and $l$ are the internal and external characteristic length of the nanostructures, respectively.

However, the integral constitutive relation in equation (4) makes the elasticity problems difficult to solve, in addition to possible lack of determinism. Eringen (1983) discussed in detail properties of non-local kernel $\alpha(|x' - x|)$ and proved that when a kernel takes a Green's function of linear differential operator:

$$\mathcal{L}\alpha(|x' - x|) = \delta(|x' - x|). \tag{5}$$

By matching the dispersion curves with lattice models, Eringen (1983) proposed a nonlocal model with the linear differential operator $\mathcal{L}$ defined as:

$$\mathcal{L} = 1 - (e_0 a)^2\nabla^2, \tag{6}$$

where $\nabla^2$ is the Laplacian operator. Therefore, the constitutive relations given by equation (4) for nonlocal elasticity can be represented by differentiable form as:

$$\sigma_{ij} - (e_0\, a)^2\nabla^2\sigma_{ij} = C_{ijkl}\varepsilon_{kl} - e_{kij}E_k - C_{ijkl}\alpha_{kl}\Delta T, \tag{7a}$$

$$D_i - (e_0\, a)^2\nabla^2 D_i = e_{ikl}\varepsilon_{kl} + k_{ik}E_k + p_i\Delta T. \tag{7b}$$

The parameter $e_0 a$ is the scale coefficient revealing the small scale effect on the responses of structures of nanosize. The value of the small-scale parameter depends on boundary condition, chirality, mode shapes, number of walls, and the nature of motions. The parameter $e_0 = (\pi^2 - 4)^{1/2}/2\pi \cong 0.39$ was given by Eringen (1983). Also, Zhang *et al* (2005) found the value of 0.82 nm for nonlocal parameter when they compared the vibrational results of simply supported single-walled CNTs with molecular dynamics simulations. The nonlocal parameter, $\mu = (e_0 a)^2$, is experimentally obtained for various materials; for instance, a conservative estimate of $\mu < 4\ (\mathrm{nm})^2$ for a single-walled CNT is proposed (Wang 2005). It is worthy to mention that this value is also chirality and size dependent, because the material properties of CNTs are widely acknowledged to be chirality dependent. There is no rigorous study made on estimating the value of small scale to simulate mechanical behavior of functionally graded micro/nanobeams (Eltaher *et al* 2013, Nazemnezhad and Hosseini-Hashemi 2014, Niknam and Aghdam 2015). Hence all researchers who worked on size-dependent mechanical behavior of FG nanobeams based on the nonlocal elasticity method investigated the effect of small scale parameter on mechanical behavior of FG nanobeams by changing the value of the small scale parameter. In the present study, a conservative estimate of the small-scale parameter is considered to be in the range of 0–4 $(\mathrm{nm})^2$ (Eltaher *et al* 2013, Nazemnezhad and Hosseini-Hashemi 2014).

### *2.3. Nonlocal FG piezoelectric nanobeam model*

According to the Timoshenko beam theory, the displacements at any point of the beam, i.e. $u_x$ and $u_z$ along $x$ and $z$ directions, respectively, are assumed to be of the form:

$$u_x(x, z, t) = u(x, t) + z\psi(x, t) \tag{8a}$$

$$u_z(x, z, t) = w(x, t) \tag{8b}$$

in which $u$ and $w$ are displacement components in the mid-plane along the coordinates $x$ and $z$, respectively, while $\psi$ denotes the total bending rotation of the cross-section and $t$ is the time.

In order to satisfy Maxwell's equation in the quasi-static approximation, the distribution of electric potential along the thickness direction is assumed to vary as a combination of a cosine and linear variation which was proposed by (Wang 2002), as follows:

$$\Phi(x, z, t) = -\cos(\beta z)\phi(x, t) + \frac{2z}{h}V_E, \tag{9}$$

where $\beta = \pi/h$. Also, $V_E$ is the initial external electric voltage applied to the FGP nanobeam; and $\phi\ (x, t)$ is the spatial function of the electric potential in the $x$-direction.

Considering strain–displacement relationships on the basis of Timoshenko beam theory, the non-zero strains can be written as:

$$\varepsilon_{xx} = \frac{\partial u}{\partial x} + z\frac{\partial\psi}{\partial x}, \tag{10}$$

$$\gamma_{xz} = \frac{\partial w}{\partial x} + \psi, \tag{11}$$

where $\varepsilon_{xx}$ and $\gamma_{xz}$ are the normal and shear components of strain tensor, respectively. Based on the assumed electric potential in equation (9), the non-zero components of electric field ($E_x$, $E_z$) can be obtained as:

$$E_x = -\Phi_{,x} = \cos(\beta z)\frac{\partial\phi}{\partial x}, \quad E_z = -\Phi_{,z} = -\beta\sin(\beta z)\phi - \frac{2V_E}{h}. \tag{12}$$

In order to obtain the governing equations, the Hamilton's principle can be stated in a dynamic form as:

$$\int_0^t \delta\left(\Pi_S + \Pi_W\right)\mathrm{d}t = 0 \tag{13}$$

here $\Pi_S$ is strain energy and $\Pi_W$ is work done by external applied forces. The first variation of strain energy $\Pi_S$ can be calculated as:

$$\delta\,\Pi_S = \int_0^L\int_{-h/2}^{h/2}\left(\sigma_{xx}\delta\varepsilon_{xx} + \sigma_{xz}\delta\gamma_{xz} - D_x\delta E_x - D_z\delta E_z\right)\mathrm{d}z\mathrm{d}x. \tag{14}$$

Substituting equations (10)–(12) into equation (14) yields:

$$\begin{aligned}\delta\,\Pi_S = &\int_0^L\left(N_x\delta\left(\frac{\partial u}{\partial x}\right) + M_x\delta\left(\frac{\partial\psi}{\partial x}\right) + Q_x\delta\left(\psi + \frac{\partial w}{\partial x}\right)\right)\mathrm{d}x\\ &+ \int_0^L\int_{-h/2}^{h/2}\left(-D_x\cos(\beta z)\delta\left(\frac{\partial\phi}{\partial x}\right) + D_z\beta\sin(\beta z)\delta\phi\right) + \mathrm{d}z\mathrm{d}x\end{aligned} \tag{15}$$

in which $N_x$, $M_x$ and $Q_x$ are the axial force, bending moment and shear force resultants, respectively. Relations between the stress resultants and stress component used in equation (15) are defined as:

$$N_x = \int_{-h/2}^{h/2}\sigma_{xx}\mathrm{d}z, \quad M_x = \int_{-h/2}^{h/2}\sigma_{xx}z\,\mathrm{d}z, \quad Q_x = \int_{-h/2}^{h/2}K_s\,\sigma_{xz}\,\mathrm{d}z \tag{16}$$

here $K_s$ denotes the shear correction factor. In general, the shear correction factor depends not only on the material and geometric parameters but also on the load and boundary conditions. For a macroscale structure with a rectangular cross-section, it is suitable to take the shear correction factor as $5/6$. However, the shear correction factor for a macroscale structures may not be applicable to a nanoscale structure due to the size-dependent material properties. So far, no experimental or theoretical results of the shear correction factor are available for nanostructures. Therefore in the present paper, following Şimşek and Yurtcu (2013), we take the shear correction factor for the FGP nanobeams approximately as the same value $K_s = 5/6$ as that for the macroscale rectangular beams.

In addition, for a typical FGP nanobeam which has been in thermal environment for a long period of time, it is assumed that the temperature can be distributed across the thickness. Thus, three kinds of thermal loading such as uniform temperature rise (UTR), linear and nonlinear (heat conduction) temperature rises is taken into consideration. Hence, the work done due to initial thermal stresses (induced by the temperature rise) and external electric voltage, $\Pi_W$, can be written in the form:

$$\Pi_W = \frac{1}{2}\int_0^L\left[\left(N_T + N_E\right)\left(\frac{\partial w}{\partial x}\right)^2\right]\mathrm{d}x, \tag{17}$$

where $N_T$ and $N_E$ are the normal forces induced by various temperature change $\Delta T$ and external electric voltage $V_E$, respectively, which can be expressed as:

$$N_T = \int_{-h/2}^{h/2}c_{11}\alpha_1(T - T)_0\mathrm{d}z, \quad N_E = -\int_{-h/2}^{h/2}e_{31}\frac{2\,V_E}{h}\mathrm{d}z, \tag{18}$$

where $T_0$ is the reference temperature. For a FGPM nanobeam under thermo-electro-mechanical loading in the one dimensional case, the nonlocal constitutive relations (7*a*) and (7*b*) may be simplified as:

$$\sigma_{xx} - (e_0 a)^2\frac{\partial^2\sigma_{xx}}{\partial x^2} = c_{11}\varepsilon_{xx} - e_{31}E_z - c_{11}\alpha_1\Delta T, \tag{19}$$

$$\sigma_{xz} - (e_0 a)^2\frac{\partial^2\sigma_{xz}}{\partial x^2} = c_{55}\gamma_{xz} - e_{15}E_x, \tag{20}$$

$$D_x - (e_0 a)^2\frac{\partial^2 D_x}{\partial x^2} = e_{15}\gamma_{xz} + k_{11}E_x, \tag{21}$$

$$D_z - (e_0 a)^2\frac{\partial^2 D_z}{\partial x^2} = e_{31}\varepsilon_{xx} + k_{33}E_z + p_3\Delta T. \tag{22}$$

The elastic stiffness constants $c_{11}$ and $c_{55}$ are defined as follows:

$$c_{11} = \frac{E}{1 - \nu^2}, \quad c_{55} = \frac{E}{2(1 + \nu)}, \tag{23}$$

where $E$ and $\nu$ are Young's modulus and Poisson's ratio, respectively. Inserting equations (15) and (17) in equation (13) and integrating by parts, and collecting the coefficients of $\delta u$, $\delta w$, $\delta\psi$ and $\delta\phi$, the following governing equations are obtained:

$$\frac{\partial N_x}{\partial x} = 0, \tag{24a}$$

$$\frac{\partial Q_x}{\partial x} - N_{x0}\frac{\partial^2 w}{\partial x^2} = 0, \tag{24b}$$

$$\frac{\partial M_x}{\partial x} - Q_x = 0, \tag{24c}$$

$$\int_{-h/2}^{h/2}\left(\cos(\beta z)\frac{\partial D_x}{\partial x} + \beta\sin(\beta z)D_z\right)\mathrm{d}z = 0, \tag{24d}$$

where $N_{x0} = N_T + N_E$. Furthermore, the corresponding natural and essential boundary conditions are defined at $x = 0$ and $x = L$ as follows:

$$N = 0 \text{ or } u = 0 \text{ at } x = 0 \text{ and } x = L, \tag{25a}$$

$$Q = 0 \text{ or } w = 0 \text{ at } x = 0 \text{ and } x = L, \tag{25b}$$

$$M = 0 \text{ or } \psi = 0 \text{ at } x = 0 \text{ and } x = L, \tag{25c}$$

$$\int_{-h/2}^{h/2} D_x \cos(\beta z) dz = 0 \text{ or } \phi = 0 \text{ at } x = 0 \text{ and } x = L. \tag{25d}$$

By integrating equations (19)–(22), the relations between local and nonlocal force–strain, moment–strain and other necessary nonlocal relations within the FGP Timoshenko nanobeam structure are achieved as:

$$N_x - \mu \frac{\partial^2 N_x}{\partial x^2} = A_{xx} \frac{\partial u}{\partial x} + B_{xx} \frac{\partial \psi}{\partial x} + A_{31}^e \phi - N_T - N_E, \tag{26}$$

$$M_x - \mu \frac{\partial^2 M_x}{\partial x^2} = B_{xx} \frac{\partial u}{\partial x} + D_{xx} \frac{\partial \psi}{\partial x} + E_{31} \phi, \tag{27}$$

$$Q_x - \mu \frac{\partial^2 Q_x}{\partial x^2} = K_s C_{xz} \left( \frac{\partial w}{\partial x} + \psi \right) - K_s E_{15} \frac{\partial \phi}{\partial x}, \tag{28}$$

$$\int_{-h/2}^{h/2} \left\{ D_x - \mu \frac{\partial^2 D_x}{\partial x^2} \right\} \cos(\beta z) dz = E_{15} \left( \frac{\partial w}{\partial x} + \psi \right) + F_{11} \frac{\partial \phi}{\partial x}, \tag{29}$$

$$\int_{-h/2}^{h/2} \left\{ D_z - \mu \frac{\partial^2 D_z}{\partial x^2} \right\} \beta \sin(\beta z) dz = A_{31}^e \frac{\partial u}{\partial x} + E_{31} \frac{\partial \psi}{\partial x} - F_{33} \phi, \tag{30}$$

where $\mu = (e_0 a)^2$ and other quantities are defined as:

$$\left\{ A_{xx}, B_{xx}, D_{xx}, C_{xz} \right\} = \int_{-h/2}^{h/2} \left\{ c_{11}, z c_{11}, z^2 c_{11}, c_{55} \right\} dz \tag{31a}$$

$$\left\{ A_{31}^e, E_{31}, E_{15} \right\} = \int_{-h/2}^{h/2} \left\{ e_{31} \beta \sin(\beta z), z e_{31} \beta \sin(\beta z), e_{15} \cos(\beta z) \right\} dz \tag{31b}$$

$$\left\{ F_{11}, F_{33} \right\} = \int_{-h/2}^{h/2} \left\{ k_{11} \cos^2(\beta z), k_{33} \beta^2 \sin^2(\beta z) \right\} dz. \tag{31c}$$

By substituting equations (24a)–(24c), into equations (26)–(28), the explicit relations of the nonlocal normal resultant force $N_x$, bending moment $M_x$ and shear force $Q_x$ can be derived as:

$$N_x = A_{xx} \frac{\partial u}{\partial x} + B_{xx} \frac{\partial \psi}{\partial x} + A_{31}^e \phi - N_T - N_E, \tag{32}$$

$$M_x = B_{xx} \frac{\partial u}{\partial x} + D_{xx} \frac{\partial \psi}{\partial x} + E_{31} \phi + \mu \left( N_{x0} \frac{\partial^2 w}{\partial x^2} \right), \tag{33}$$

$$Q_x = K_s C_{xz} \left( \frac{\partial w}{\partial x} + \psi \right) - K_s E_{15} \frac{\partial \phi}{\partial x} + \mu \left( N_{x0} \frac{\partial^3 w}{\partial x^3} \right). \tag{34}$$

It should be pointed that substituting equation (24d) into equations (29) and (30), does not lead to the explicit expressions for $D_x$ and $D_z$ as there are two unknowns and only one equilibrium equation (24d). However, by using equations (29) and (30), equation (24d) can be re-expressed in terms of $u$, $w$, $\psi$ and $\phi$. Then, based on Timoshenko beam theory, the stability equations for a nonlocal FG piezoelectric beam can be derived by substituting for $N_x$, $M_x$ and $Q_x$ from equations (32)–(34) into equations (24a)–(24c) as follows:

$$A_{xx} \frac{\partial^2 u}{\partial x^2} + B_{xx} \frac{\partial^2 \psi}{\partial x^2} + A_{31}^e \frac{\partial \phi}{\partial x} = 0, \tag{35}$$

$$K_s C_{xz} \left( \frac{\partial^2 w}{\partial x^2} + \frac{\partial \psi}{\partial x} \right) - K_s E_{15} \frac{\partial^2 \phi}{\partial x^2} - \left( N_T + N_E \right) \frac{\partial^2 w}{\partial x^2} + \mu \left( \left( N_T + N_E \right) \frac{\partial^4 w}{\partial x^4} \right) = 0, \tag{36}$$

$$B_{xx} \frac{\partial^2 u}{\partial x^2} + D_{xx} \frac{\partial^2 \psi}{\partial x^2} + E_{31} \frac{\partial \phi}{\partial x} - K_s C_{xz} \left( \frac{\partial w}{\partial x} + \psi \right) + K_s E_{15} \frac{\partial \phi}{\partial x} = 0, \tag{37}$$

$$E_{15} \left( \frac{\partial^2 w}{\partial x^2} + \frac{\partial \psi}{\partial x} \right) + F_{11} \frac{\partial^2 \phi}{\partial x^2} + A_{31}^e \frac{\partial u}{\partial x} + E_{31} \frac{\partial \psi}{\partial x} - F_{33} \phi = 0. \tag{38}$$

**Table 1.** Thermo-electro-mechanical coefficients of material properties for PZT-4 and PZT-5H (Doroushi *et al* 2011).

| Properties | PZT-4 | PZT-5H |
|---|---|---|
| $c_{11}$ (GPa) | 81.3 | 60.6 |
| $c_{55}$ (GPa) | 25.6 | 23.0 |
| $e_{31}$ (Cm$^{-2}$) | −10.0 | −16.604 |
| $e_{15}$ (Cm$^{-2}$) | 40.3248 | 44.9046 |
| $k_{11}$ (C$^2$m$^{-2}$ N$^{-1}$) | $0.6712 \times 10^{-8}$ | $1.5027 \times 10^{-8}$ |
| $k_{33}$ (C$^2$m$^{-2}$ N$^{-1}$) | $1.0275 \times 10^{-8}$ | $2.554 \times 10^{-8}$ |
| $\alpha_1$ (K$^{-1}$) | $2.0 \times 10^{-6}$ | $10.0 \times 10^{-6}$ |
| $\kappa$ (Wm$^{-1}$ K$^{-1}$) | 2.1 | 1.5 |
| $p_3$ (Cm$^{-2}$ K$^{-1}$) | $2.5 \times 10^{-5}$ | $0.548 \times 10^{-5}$ |

## 3. Types of thermal distributions

### 3.1. Uniform temperature rise

The FGP nanobeam initial temperature is assumed to be $T_0 = 300$ K, which is a stress free state, uniformly changed to final temperature with $\Delta T$. The temperature rise is given by:

$$\Delta T = T - T_0. \tag{39}$$

### 3.2. Linear temperature rise (LTR)

Consider a graded nanobeam where the temperature of the upper surface (PZT-4-rich) is $T_u$ and it is considered to vary

**Table 2.** Comparison of the critical buckling temperature $\Delta T_{cr}$ (K) for a S–S FG nanobeam under LTR loading with various volume fraction index ($h = 0.25$ nm, $L = 10$ nm).

| | $p = 0$ | | $p = 0.5$ | | $p = 1$ | | $p = 5$ | |
|---|---|---|---|---|---|---|---|---|
| $\mu$ (nm)$^2$ | Ebrahimi and Salari (2015b) | Present | Ebrahimi and Salari (2015b) | Present | Ebrahimi and Salari (2015b) | Present | Ebrahimi and Salari (2015b) | Present |
| 0 | 127.3340 | 127.3340 | 95.5739 | 95.5739 | 84.6229 | 84.6229 | 69.4307 | 69.4307 |
| 1 | 114.9980 | 114.9980 | 86.0456 | 86.0456 | 76.0818 | 76.0818 | 62.2798 | 62.2798 |
| 2 | 104.6950 | 104.6950 | 78.0881 | 78.0881 | 68.9486 | 68.9486 | 56.3077 | 56.3077 |
| 3 | 95.9606 | 95.9606 | 71.3424 | 71.3424 | 62.9019 | 62.9019 | 51.2452 | 51.2452 |
| 4 | 88.4628 | 88.4628 | 65.5514 | 65.5514 | 57.7108 | 57.7108 | 46.8992 | 46.8992 |

**Table 3.** Critical buckling temperature $\Delta T_{cr}$ (K) of a S–S FGP nanobeam under UTR loading for various values of applied electric voltage and material graduation parameter.

| | | $L/h = 20$ | | | $L/h = 25$ | | | $L/h = 30$ | | |
|---|---|---|---|---|---|---|---|---|---|---|
| | | Gradient index | | | Gradient index | | | Gradient index | | |
| $\mu$ (nm)$^2$ | $V_E$ (V) | 0.2 | 0.5 | 1 | 0.2 | 0.5 | 1 | 0.2 | 0.5 | 1 |
| | −0.5 | 778.8150 | 575.7340 | 464.4990 | 551.8580 | 412.9180 | 337.0003 | 438.2060 | 332.5280 | 274.9660 |
| 0 | 0 | 692.1630 | 503.5370 | 399.9110 | 443.5440 | 322.6720 | 256.2650 | 308.2290 | 224.2320 | 178.0840 |
| | +0.5 | 605.5120 | 431.3390 | 335.3220 | 335.2300 | 232.4250 | 175.5290 | 178.2520 | 115.9370 | 81.2009 |
| | −0.5 | 716.6380 | 530.5010 | 428.5750 | 512.0150 | 383.9330 | 313.9800 | 410.5180 | 312.3850 | 258.9690 |
| 1 | 0 | 629.9860 | 458.3040 | 363.9870 | 403.7002 | 293.6860 | 233.2440 | 280.5410 | 204.0900 | 162.0860 |
| | +0.5 | 543.3350 | 386.1070 | 299.3980 | 295.3860 | 203.4400 | 152.5090 | 150.5630 | 95.7937 | 65.2036 |
| | −0.5 | 664.7100 | 492.7250 | 398.5730 | 478.7390 | 359.7250 | 294.7550 | 387.3940 | 295.5630 | 245.6090 |
| 2 | 0 | 578.0590 | 420.5280 | 333.9850 | 370.4250 | 269.4790 | 214.0190 | 257.4170 | 187.2670 | 148.7260 |
| | +0.5 | 491.4080 | 348.3310 | 269.3960 | 262.1110 | 179.2320 | 133.2830 | 127.4400 | 78.9715 | 51.8435 |
| | −0.5 | 620.6920 | 460.7020 | 373.1410 | 450.5320 | 339.2050 | 278.4570 | 367.7920 | 281.3030 | 234.2840 |
| 3 | 0 | 534.0400 | 388.5050 | 308.5520 | 342.2170 | 248.9580 | 197.7220 | 237.8150 | 173.0070 | 137.4010 |
| | +0.5 | 447.3890 | 316.3080 | 243.9640 | 233.9030 | 158.7120 | 116.9860 | 107.8380 | 64.7112 | 40.5181 |
| | −0.5 | 582.9030 | 433.2110 | 351.3070 | 426.3160 | 321.5880 | 264.4660 | 350.9640 | 269.0610 | 224.5610 |
| 4 | 0 | 496.2510 | 361.0140 | 286.7190 | 318.0020 | 231.3420 | 183.7310 | 220.9870 | 160.7650 | 127.6780 |
| | +0.5 | 409.5997 | 288.8170 | 222.1300 | 209.6880 | 141.0950 | 102.9950 | 91.0096 | 52.4691 | 30.7955 |

**Table 4.** Critical buckling temperature $\Delta T_{cr}$ (K) of a S–S FGP nanobeam under LTR loading for various values of applied electric voltage and material graduation parameter.

| | | $L/h = 20$ | | | $L/h = 25$ | | | $L/h = 30$ | | |
|---|---|---|---|---|---|---|---|---|---|---|
| | | Gradient index | | | Gradient index | | | Gradient index | | |
| $\mu$ (nm)$^2$ | $V_E$ (V) | 0.2 | 0.5 | 1 | 0.2 | 0.5 | 1 | 0.2 | 0.5 | 1 |
| | −0.5 | 1840.4103 | 1411.3847 | 1119.9276 | 1300.6258 | 1008.7531 | 809.1771 | 1030.3200 | 809.9543 | 657.9830 |
| 0 | 0 | 1634.3219 | 1232.8460 | 962.5075 | 1043.0154 | 785.5797 | 612.4019 | 721.1875 | 542.1463 | 421.8528 |
| | +0.5 | 1428.2336 | 1054.3074 | 805.0874 | 785.4050 | 562.4064 | 415.6268 | 412.0550 | 274.3383 | 185.7227 |
| | −0.5 | 1692.5306 | 1299.5272 | 1032.3707 | 1205.8633 | 937.0736 | 753.0702 | 964.4674 | 760.1425 | 618.9932 |
| 1 | 0 | 1486.4423 | 1120.9886 | 874.9506 | 948.2529 | 713.9003 | 556.2951 | 655.3349 | 492.3345 | 382.8630 |
| | +0.5 | 1280.3540 | 942.4499 | 717.5304 | 690.6425 | 490.7269 | 359.5199 | 346.2024 | 224.5264 | 146.7328 |
| | −0.5 | 1569.0292 | 1206.1096 | 959.2477 | 1126.7226 | 877.2106 | 706.2126 | 909.4706 | 718.5422 | 586.4309 |
| 2 | 0 | 1362.9408 | 1027.5710 | 801.8275 | 869.1122 | 654.0373 | 509.4375 | 600.3382 | 450.7342 | 350.3007 |
| | +0.5 | 1156.8525 | 849.0323 | 644.4074 | 611.5018 | 430.8639 | 312.6623 | 291.2057 | 182.9262 | 114.1706 |
| | −0.5 | 1464.3368 | 1126.9194 | 897.2612 | 1059.6349 | 826.4646 | 666.4914 | 862.8498 | 683.2776 | 558.8278 |
| 3 | 0 | 1258.2485 | 948.3807 | 739.8411 | 802.0245 | 603.2913 | 469.7163 | 553.7173 | 415.4696 | 322.6976 |
| | +0.5 | 1052.1601 | 769.8420 | 582.4209 | 544.4141 | 380.1179 | 272.9411 | 244.5849 | 147.6616 | 86.5675 |
| | −0.5 | 1374.4606 | 1058.9363 | 844.0471 | 1002.0415 | 782.9003 | 632.3916 | 822.8269 | 653.0037 | 535.1311 |
| 4 | 0 | 1168.3723 | 880.3976 | 686.6270 | 744.4311 | 559.7270 | 435.6164 | 513.6944 | 385.1957 | 299.0010 |
| | +0.5 | 962.2840 | 701.8589 | 529.2069 | 486.8207 | 336.5536 | 238.8413 | 204.5619 | 117.3877 | 62.8708 |

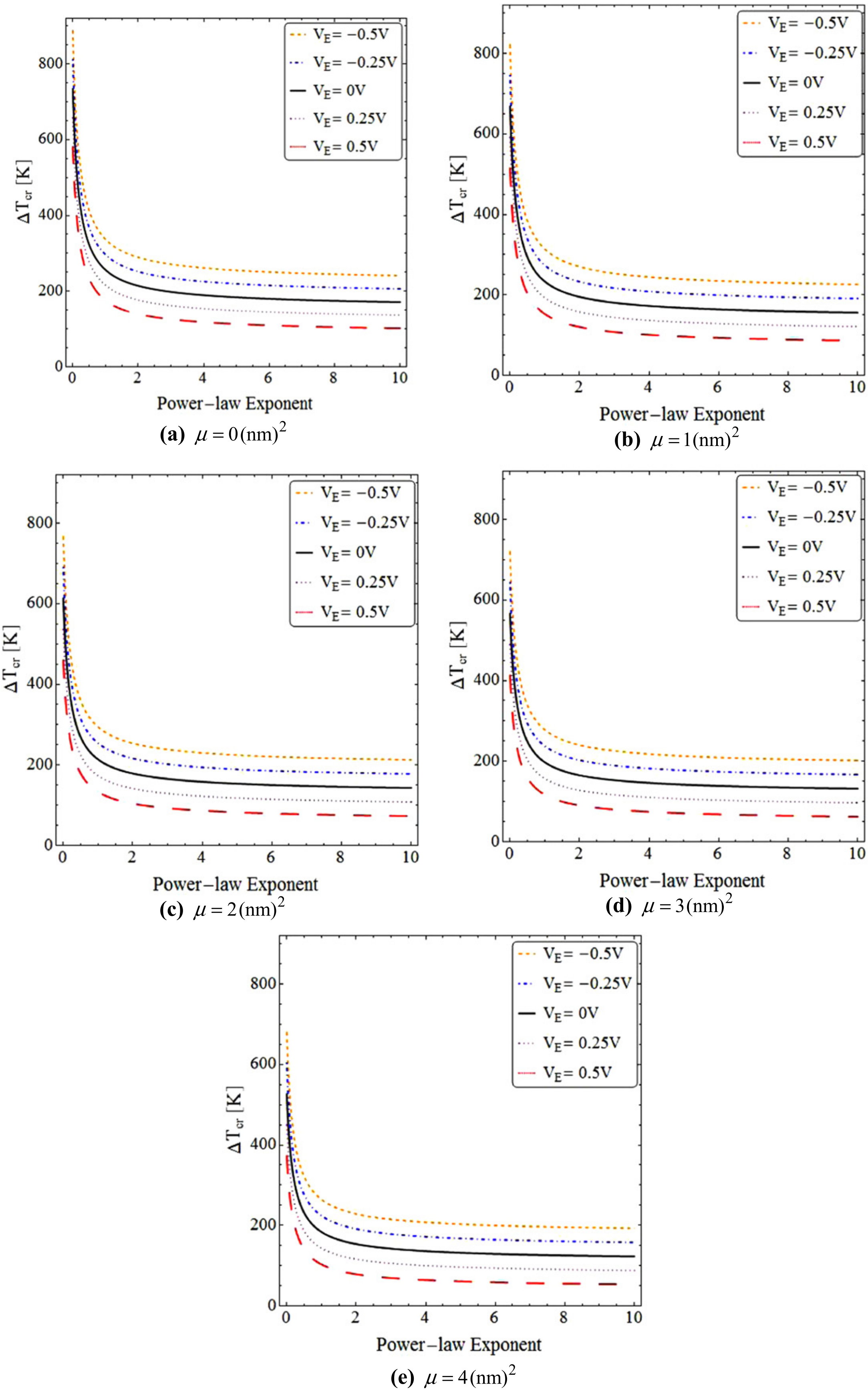


**Figure 2.** Variations of the uniform critical buckling temperature of the S–S FGP nanobeam against power-law exponent for different values of nonlocal parameters and external electric voltage ($L/h = 25$).

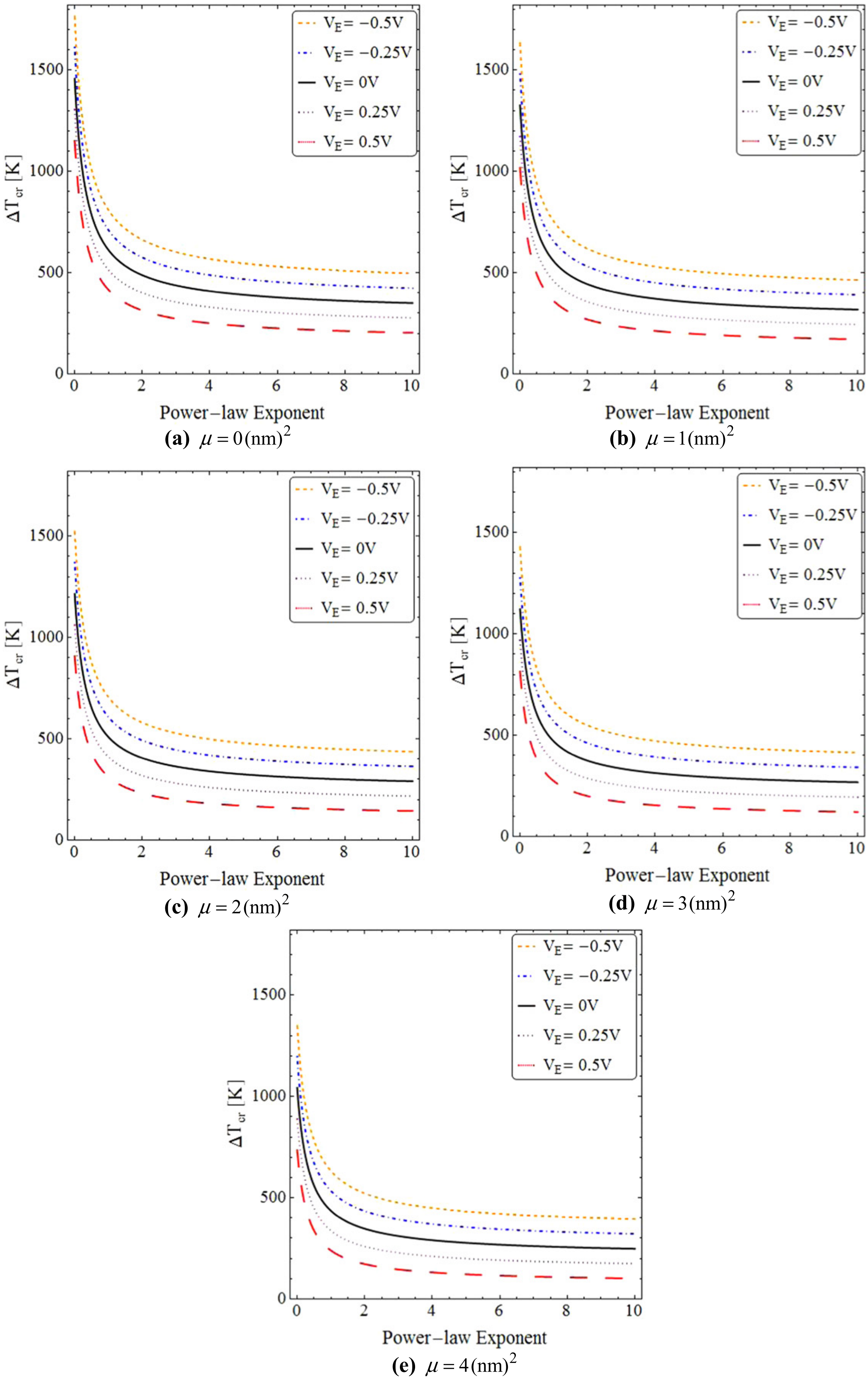


**Figure 3.** Variations of the linear critical buckling temperature of the S–S FGP nanobeam against power-law exponent for different values of nonlocal parameters and external electric voltage ($L/h = 25$).

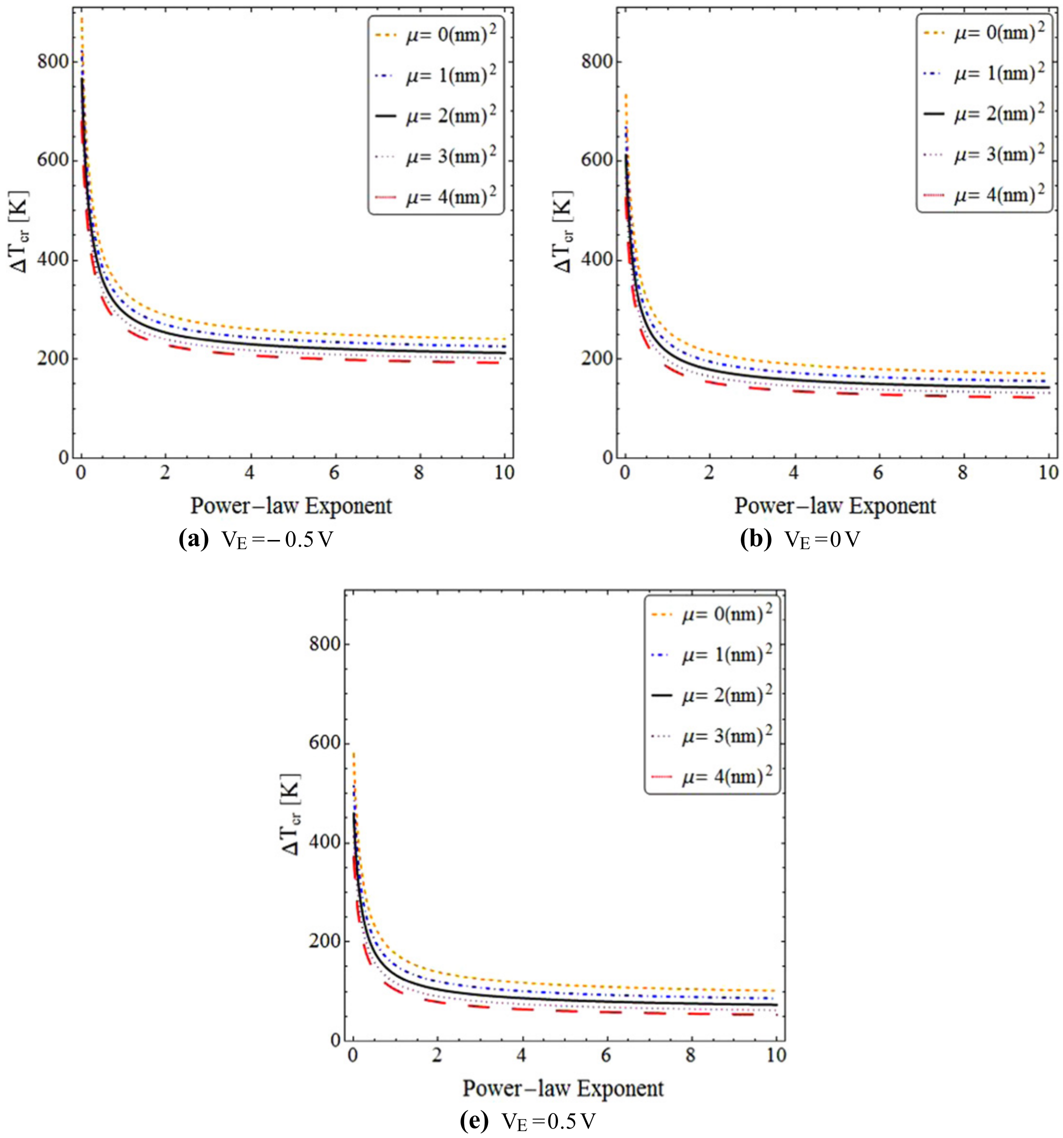


**Figure 4.** Variations of the uniform critical buckling temperature of the S–S FGP nanobeam against power-law exponent for different values of external electric voltage and nonlocal parameters ($L/h = 25$).

linearly along the thickness from $T_u$ to the lower surface (PZT-5H-rich) temperature $T_l$. Therefore, the temperature rise as a function of thickness is considered as below (Kiani and Eslami 2013):

$$T = T_l + \Delta T\left(\frac{1}{2} + \frac{z}{h}\right). \tag{40}$$

The $\Delta T$ in equation (40) could be defined $\Delta T = T_u - T_l$.

### 3.3. Nonlinear temperature rise

In such a case, NLTR across the thickness is assumed. The steady-state one-dimensional heat conduction equation with the known temperature boundary conditions on bottom and top surfaces of the FGP nanobeam can be obtained by solving the following equation (Zhang 2013):

$$-\frac{\mathrm{d}}{\mathrm{d}z}\left(\kappa(z)\frac{\mathrm{d}\,T}{\mathrm{d}z}\right) = 0$$
$$T\left(\frac{h}{2}\right) = T_u, \quad T\left(-\frac{h}{2}\right) = T_l, \tag{41}$$

where $\kappa$ is the thermal conductivity coefficient. The solution of equation (41) subjected to the boundary conditions can be solved by the following equation:

$$T = T_l + (\Delta T)\frac{\int_{-h/2}^{z}\frac{1}{\kappa(z)}\mathrm{d}z}{\int_{-h/2}^{h/2}\frac{1}{\kappa(z)}\mathrm{d}z}, \tag{42}$$

where $\Delta T = T_u - T_l$.

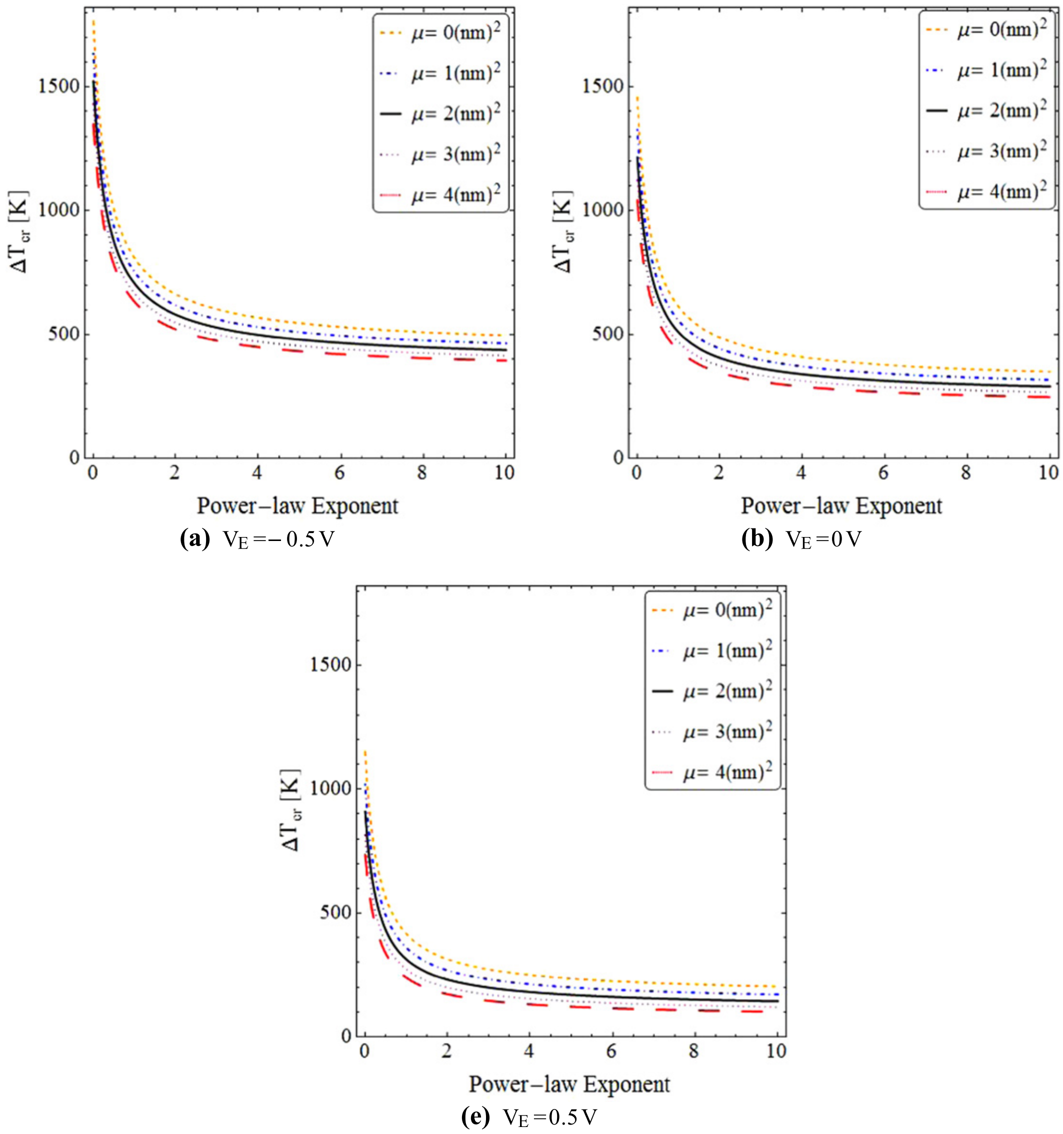


**Figure 5.** Variations of the linear critical buckling temperature of the S–S FGP nanobeam against power-law exponent for different values of external electric voltage and nonlocal parameters ($L/h = 25$).

## 4. Solution procedure

In this section, the analytical solutions of the stability equations for thermal buckling of FGPM nanobeam with simply supported (S–S) boundary conditions are derived by using Navier method. Also, it is assumed that the value of electric potential is equal to zero at the ends of the FGPM nanobeam. The displacement functions are expressed as product of undetermined coefficients and known trigonometric functions to satisfy the governing equations and the conditions at $x = 0, L$. The following displacement fields are assumed to be of the form:

$$u(x, t) = \sum_{n=1}^{\infty} U_n \cos\left(\frac{n\pi}{L}x\right) \mathrm{e}^{\,\mathrm{i}\omega_n t}, \tag{43}$$

$$w(x, t) = \sum_{n=1}^{\infty} W_n \sin\left(\frac{n\pi}{L}x\right) \mathrm{e}^{\,\mathrm{i}\omega_n t}, \tag{44}$$

$$\psi(x, t) = \sum_{n=1}^{\infty} \Psi_n \cos\left(\frac{n\pi}{L}x\right) \mathrm{e}^{\,\mathrm{i}\omega_n t}, \tag{45}$$

$$\phi(x, t) = \sum_{n=1}^{\infty} \Phi_n \sin\left(\frac{n\pi}{L}x\right) \mathrm{e}^{\,\mathrm{i}\omega_n t}, \tag{46}$$

where $U_n$, $W_n$, $\Psi_n$ and $\Phi_n$ are the unknown Fourier coefficients to be determined for each $n$ value. The boundary conditions for simply supported FGP beam can be identified as:

$$u(0) = 0, \quad \frac{\partial u}{\partial x}(L) = 0, \quad w(0) = w(L) = 0,$$
$$\frac{\partial \psi}{\partial x}(0) = \frac{\partial \psi}{\partial x}(L) = 0, \quad \phi(0) = \phi(L) = 0. \tag{47}$$

**Table 5.** Critical buckling temperature $\Delta T_{cr}$ (K) of a S–S FGP nanobeam under NLTR loading for various values of applied electric voltage and material graduation parameter.

| $\mu\,(\mathrm{nm})^2$ | $V_E\,(V)$ | $L/h=20$ | | | $L/h=25$ | | | $L/h=30$ | | |
|---|---|---|---|---|---|---|---|---|---|---|
| | | Gradient index | | | Gradient index | | | Gradient index | | |
| | | 0.2 | 0.5 | 1 | 0.2 | 0.5 | 1 | 0.2 | 0.5 | 1 |
| | −0.5 | 1789.8671 | 1337.7685 | 1046.7175 | 1264.9068 | 956.1376 | 756.2808 | 1002.0244 | 767.7080 | 614.9704 |
| 0 | 0 | 1589.4386 | 1168.5422 | 899.5880 | 1014.3711 | 744.6048 | 572.3690 | 701.3816 | 513.8685 | 394.2761 |
| | +0.5 | 1389.0101 | 999.3159 | 752.4585 | 763.8355 | 533.0719 | 388.4571 | 400.7388 | 260.0291 | 173.5819 |
| | −0.5 | 1646.0487 | 1231.7453 | 964.8842 | 1172.7468 | 888.1969 | 703.8417 | 937.9802 | 720.4943 | 578.5294 |
| 1 | 0 | 1445.6202 | 1062.5190 | 817.7547 | 922.2111 | 676.6640 | 519.9298 | 637.3374 | 466.6548 | 357.8351 |
| | +0.5 | 1245.1916 | 893.2927 | 670.6252 | 671.6754 | 465.1311 | 336.0179 | 336.6946 | 212.8154 | 137.1408 |
| | −0.5 | 1525.9390 | 1143.2003 | 896.5413 | 1095.7795 | 831.4563 | 660.0472 | 884.4939 | 681.0639 | 548.0957 |
| 2 | 0 | 1325.5104 | 973.9740 | 749.4118 | 845.2438 | 619.9234 | 476.1354 | 583.8511 | 427.2244 | 327.4014 |
| | +0.5 | 1125.0819 | 804.7477 | 602.2823 | 594.7081 | 408.3905 | 292.2235 | 283.2083 | 173.3850 | 106.7072 |
| | −0.5 | 1424.1218 | 1068.1405 | 838.6068 | 1030.5342 | 783.3572 | 622.9226 | 839.1534 | 647.6386 | 522.2970 |
| 3 | 0 | 1223.6932 | 898.9142 | 691.4773 | 779.9985 | 571.8243 | 439.0107 | 538.5106 | 393.7992 | 301.6028 |
| | +0.5 | 1023.2647 | 729.6879 | 544.3478 | 529.4628 | 360.2914 | 255.0988 | 237.8678 | 139.9597 | 80.9085 |
| | −0.5 | 1336.7139 | 1003.7034 | 788.8714 | 974.5225 | 742.0651 | 591.0519 | 800.2296 | 618.9438 | 500.1494 |
| 4 | 0 | 1136.2854 | 834.4771 | 641.7419 | 723.9868 | 530.5323 | 407.1400 | 499.5868 | 365.1043 | 279.4552 |
| | +0.5 | 935.8568 | 665.2507 | 494.6124 | 473.4511 | 318.9994 | 223.2281 | 198.9440 | 111.2649 | 58.7609 |

Substituting equations (43)–(46) into equations (35)–(38) respectively, leads to equations (48)–(51):

$$\left(-A_{xx}\left(\frac{n\pi}{L}\right)^2\right)U_n + \left(-B_{xx}\left(\frac{n\pi}{L}\right)^2\right)\Psi_n + \left(A_{31}^e\left(\frac{n\pi}{L}\right)\right)\Phi_n = 0, \tag{48}$$

$$\left(-K_sC_{xz}\left(\frac{n\pi}{L}\right)^2 + (N_T+N_E)\left(\frac{n\pi}{L}\right)^2 \times\left(1+\mu\left(\frac{n\pi}{L}\right)^2\right)\right)W_n - \left(K_sC_{xz}\left(\frac{n\pi}{L}\right)\right)\Psi_n + \left(K_sE_{15}\left(\frac{n\pi}{L}\right)^2\right)\Phi_n = 0, \tag{49}$$

$$\left(-B_{xx}\left(\frac{n\pi}{L}\right)^2\right)U_n - \left(K_sC_{xz}\left(\frac{n\pi}{L}\right)\right)W_n + \left(-D_{xx}\left(\frac{n\pi}{L}\right)^2 - K_sC_{xz}\right)\Psi_n + \left(E_{31}\left(\frac{n\pi}{L}\right) + K_sE_{15}\left(\frac{n\pi}{L}\right)\right)\Phi_n = 0, \tag{50}$$

$$\left(-A_{31}^e\left(\frac{n\pi}{L}\right)\right)U_n - \left(E_{15}\left(\frac{n\pi}{L}\right)^2\right)W_n - \left(E_{15}\left(\frac{n\pi}{L}\right) + E_{31}\left(\frac{n\pi}{L}\right)\right)\Psi_n - \left(F_{11}\left(\frac{n\pi}{L}\right)^2 + F_{33}\right)\Phi_n = 0. \tag{51}$$

By setting the determinant of the coefficient matrix of the above equations, the nontrivial analytical solutions can be obtained from the following equations:

$$\left\{\left([K] + \Delta T\left[K_T\right]\right)\right\}\begin{Bmatrix} U_n \\ W_n \\ \Psi_n \\ \Phi_n \end{Bmatrix} = 0, \tag{52}$$

where $[K]$ and $[K_T]$ are stiffness matrix and the coefficient matrix of temperature change, respectively. By setting this polynomial to zero, we can find critical buckling temperature $\Delta T_{cr}$ of the FGP nanobeam subjected to thermo-electrical loading.

## 5. Results and discussion

In this section, the thermal buckling of an FGPM nanobeam under various thermal loading is investigated through some numerical examples. Also, to demonstrate the applied electric voltage and nonlocal parameter effects on the thermal buckling analysis of FGP nanobeams, variations of the critical buckling temperatures versus external electric voltage, power law index, and thickness ratios of the FG piezoelectric nanobeam, are presented in this section. Most studies in previous literature are concerned with the case that assumes the small scale parameter is independent to the volume fractions of the material constituents. It is noted that since the small scale parameter $e_0\,a$ is a material property differing from one material to another, assuming $e_0\,a$ to be constant through the thickness is a simplifying assumption considered in the present study. Also, it should be pointed out that to evaluate the length scale parameter of a FG nanobeam, the experimental data is needed. However, so far, there is no available experimental data relevant to the FG nanobeams in open literature. In order to quantitatively analyze the size effect on the thermal buckling of nanobeams, the values of

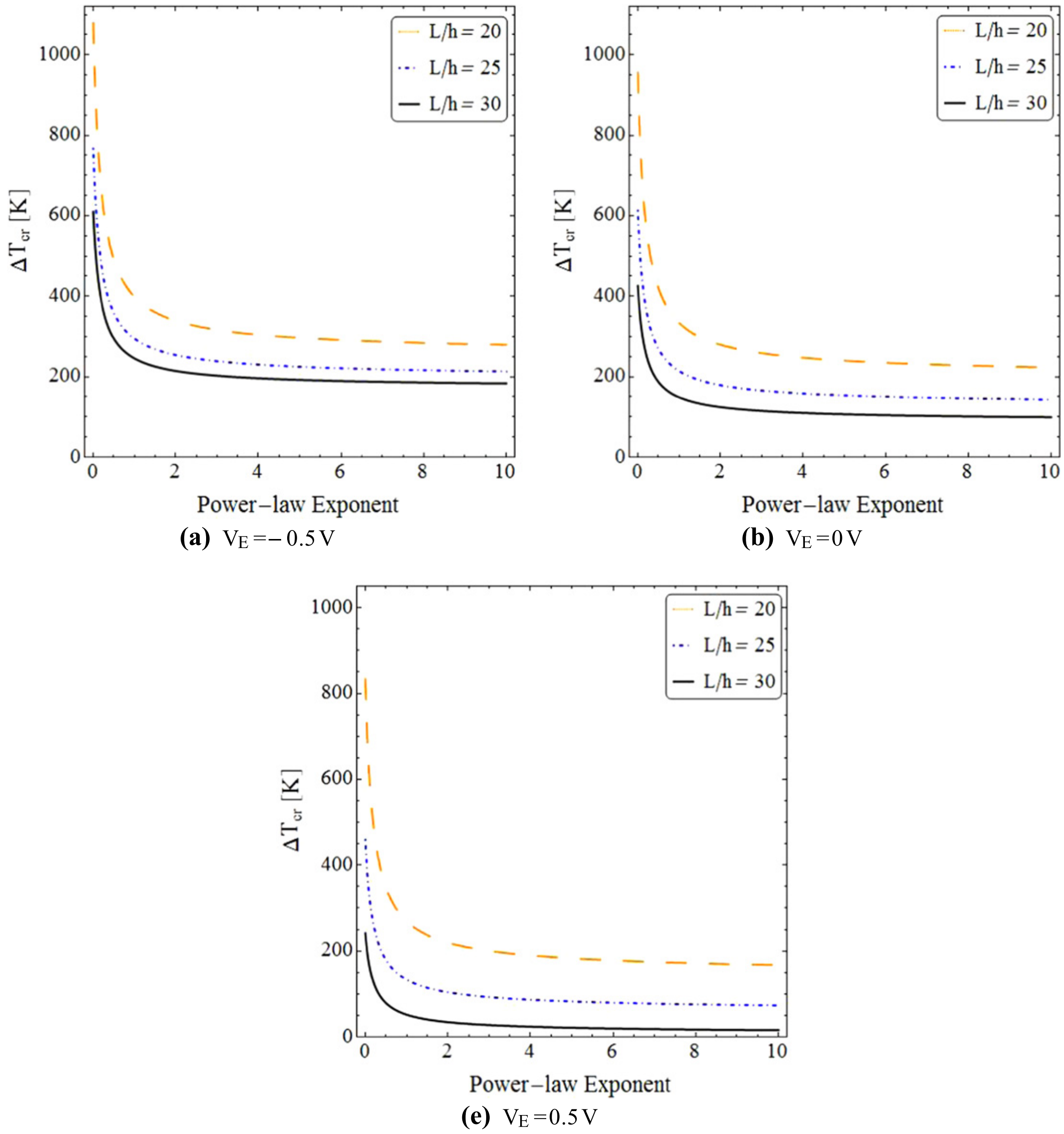


**Figure 6.** Variations of the uniform critical buckling temperature of the S–S FGP nanobeam against power-law exponent for different values of aspect ratio and external electric voltage ($\mu = 2\ (\mathrm{nm})^2$).

nonlocal parameter for the FG nanobeams is assumed to be constant in the following numerical results. To this end, the nonlocal FGP beam made of PZT-4 and PZT-5H, with thermo-electro-mechanical material properties listed in table 1, is considered. The bottom surface of the graded nanobeam is PZT-5H rich, whereas the top surface of the beam is PZT-4 rich. The beam geometry has the following dimensions: $L$ (length) $= 10$ nm and $h$ (thickness) $=$ varied. Also, it is assumed that the temperature increase in lower surface to reference themperature $T_0$ of the FGP nanobeam is $T_l - T_0 = 5$ K (Kiani and Eslami 2013).

The numerical or analytical results for the thermoelectrically buckling behavior of FGP nanobeam based on the nonlocal elasticity theory are not available in the literature. When no piezoelectric effect being taken into account, equations (35)–(38) reduce to the model for FG nanobeam based on nonlocal elasticity theory. As part of the validation of the present method, a comparison study is performed to check the reliability of the present method and formulation. For this purpose, the FG nanobeam consists of SUS 304 and $Si_3N_4$ is considered. In table 2, the critical buckling temperatures of S–S FG nanobeams are compared with those of Ebrahimi and Salari (2015b) which has been obtained by analytical solution for various values of the gradient index and nonlocality parameter. It is obvious from table 2 that there is good agreement between the two results.

After extensive validation of the present formulation, the effects of different parameters such as external electric voltage, various temperature rise, nonlocality and gradient index on buckling behavior of FGP nanobeam are investigated. The effect of the external electric voltage ($V_E$), gradient index ($p$), aspect ratio ($L/h$) and nonlocal parameter ($\mu$) on the thermal buckling behavior of the S–S graded piezoelectric nanobeam based on analytical Navier solution method is examined and scrutinized in tables 3 and 4 that list the variation of the critical buckling temperature of FGP nanobeam subjected to

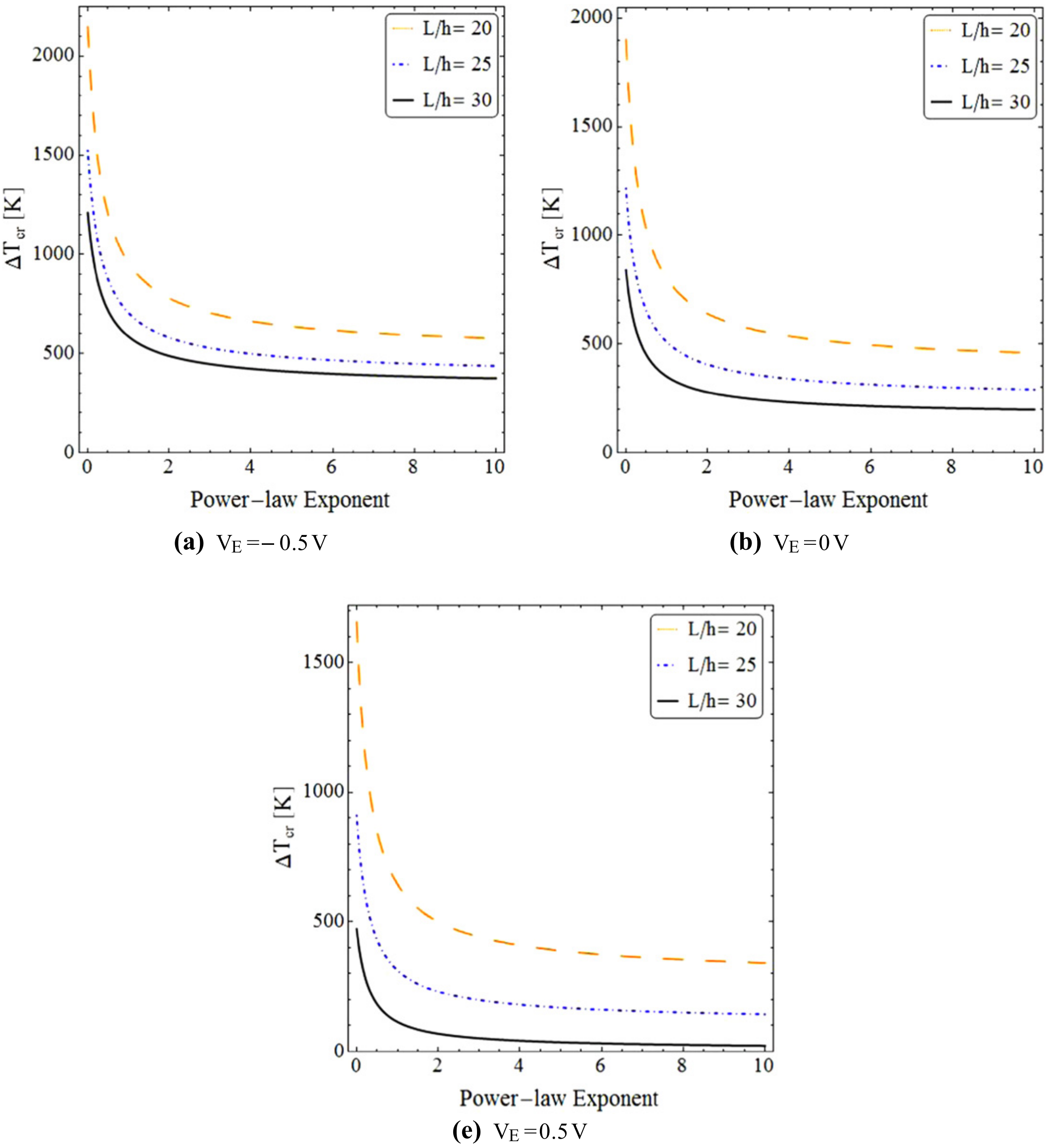


**Figure 7.** Variations of the linear critical buckling temperature of the S–S FGP nanobeam against power-law exponent for different values of aspect ratio and external electric voltage ($\mu = 2$ (nm)$^2$).

uniform (UTR) and LTRs, respectively. It is evident from the results of the tables that increasing the nonlocality parameter yields the reduction in buckling temperature for every material graduation and thermal loading, which these observations mean that the small scale effects in the nonlocal model make FGP nanobeams more flexible. One important observation within the range of the critical temperature, it is clear that the FGP nanobeams with negative value of applied voltage usually provide larger values of the buckling temperature results. In addition, it is indicated that increase the power indexes lead to a decrease of the $\Delta T_{\mathrm{cr}}$. This is because that as increasing the value of gradient index the percentage of PZT-5H phase will rise, thus making such FGP nanobeams more flexible. At the same time, there is no available data for the critical buckling temperature of FGP nanobeams as far as the author knows. Therefore, it is believed that the tabulated results can be useful reference for future studies.

The buckling temperature difference parameter versus gradient index ($p$) is presented in figures 2 and 3 for the UTR and LTR cases of thermal loading, respectively. In these figures, the critical temperature of simply supported FGPM nanobeam is plotted as a function of the external electric voltage for the selected values of the the nonlocal parameter ($\mu = 0, 1, 2, 3, 4$) at constant slenderness ratio $L/h = 25$. It is seen that the positive and negative electric voltage respectively decreases and increases the critical buckling temperature. The reason is that compressive and tensile in-plane forces are generated in the graded nanobeams by imposing positive and negative voltages, respectively. In addition, it is observed that the critical temperature of FGP nanobeam decreases with the increase of small scale parameter. This is due to the reduction in total stiffness of the beam, since geometrical stiffness decreases when nonlocal parameter rises.

But in order to clarify the effect of the small scale parameter and applied electric voltage on the buckling analysis, figures 4 and 5 intuitively exhibit the variations of the critical temperature difference of nonlocal FGP beam with respect to uniform and linear thermal loadings for different values of nonlocal parameter and electric voltage at constant slenderness ratio $L/h = 25$. Observing these figures, it is easily deduced for both cases of thermal loading that, the buckling temperature reduce with high rate where the power exponent in range from 0 to 2 than that where power exponent in range between 2 and 10. However, the above results obtained also show that the critical temperature of the nonlocal FGP model are always smaller than those of the classical graded piezoelectric beam model. With the increase the nonlocal parameter $\mu$ from 0 to 4 $(\mathrm{nm})^2$, the $\Delta T_{\mathrm{cr}}$ decrease significantly. The results indicate that the nonlocal effect is tending to weaken the stiffness of nanostructures and hence decreases the buckling temperatures.

The critical buckling temperatures of size-dependent FGPM nanobeam under NLTR loading for various aspect ratio parameter, nonlocal coefficients, power-law exponent and three cases of electrical loading are summarized in table 5. The similar conclusions are derived from this table for the effect of the electric voltage parameter on the critical buckling temperature. It can be concluded from table 5 that the buckling temperature decreases when the gradient index increases. On the other hand, this table reveal that the critical temperature magnifies with the decrease of the power-law exponent parameter. It can also be seen that the critical buckling temperatures predicted by UTR are always smaller than those evaluated by LTR and NLTR and this situation is more prominent for smaller nonlocality parameter. In addition, it can be emphasized that the buckling temperatures decrease depending on an increment in material property gradient index and small scale parameter.

Finally, effects of changing length-to-thickness ratio $(L/h)$ on the thermal buckling behavior of FGP nanobeam for different values of electric voltage and two types of thermal loading are investigated in figures 6 and 7. In all figures, results are prepared for $\mu = 2\ (\mathrm{nm})^2$. Regardless of the type of thermal loadings, it can be pointed that the values of critical temperature difference decrease with the increasing value of the aspect ratio at a constant material distribution. That is because a higher length-to-thickness ratio indicates that the FGPM nanobeam is thinner with a lower stiffness.

## 6. Conclusions

This study focuses on the thermo-electrical buckling of a size-dependent FGP nanobeam by using Timoshenko beam theory and Eringen's nonlocal elasticity theory. The governing differential equations and related boundary conditions are derived by implementing Hamilton's principle. The Navier solution method is adopted to obtain the analytical solutions of the stability equations. Thermo-electro-mechanical properties of the FGP nanobeams are assumed to be function of thickness and based on power-law model.

Validity of applied procedure is verified through comparison with previous works and analytical solution for thermal buckling of FG nanobeams. Finally, through some parametric study and numerical examples, the effect of different parameters are investigated for graded piezoelectric nanobeams in different set of thermal loading. As shown in several numerical exercises, it is revealed that many parameters such as external electric voltage, small scale parameter, power-law gradient index, various thermal loading and aspect ratio have significant impact on critical buckling temperature of FGP nanobeams. As previously specified, increasing the nonlocal parameter yields the decrease in critical temperatures for every types of thermal environments. However, the FGP nanobeam model produces smaller buckling temperature than the classical beam model. Therefore, the small scale effects should be considered in the analysis of mechanical behavior of nanostructures. The results indicated that the dramatic reduction in critical temperature differences of the nonlocal FGP beam is detected as the increase of the power-law index. Also, it was observed that the effects of external electric voltages on buckling behavior of graded nanobeam are dependent on their sign.

## References


Akgöz B and Civalek Ö 2014 Thermo-mechanical buckling behavior of functionally graded microbeams embedded in elastic medium *Int. J. Eng. Sci.* **85** 90–104

Bodaghi M, Damanpack A, Aghdam M and Shakeri M 2014 Geometrically nonlinear transient thermo-elastic response of FG beams integrated with a pair of FG piezoelectric sensors *Compos. Struct.* **107** 48–59

Carbonari R C, Silva E C and Paulino G H 2009 Multi-actuated functionally graded piezoelectric micro-tools design: a multiphysics topology optimization approach *Int. J. Numer. Methods Eng.* **77** 301–36

Doroushi A, Eslami M and Komeili A 2011 Vibration analysis and transient response of an FGPM beam under thermo-electro-mechanical loads using higher-order shear deformation theory *J. Intell. Mater. Syst. Struct.* **22** 231–43

Ebrahimi F and Rastgo A 2008 An analytical study on the free vibration of smart circular thin FGM plate based on classical plate theory. *Thin-Walled Struct.* **46** 1402–8

Ebrahimi F, Rastgoo A and Atai A 2009 A theoretical analysis of smart moderately thick shear deformable annular functionally graded plate *Eur. J. Mech.* A **28** 962–73

Ebrahimi F and Salari E 2015a Thermo-mechanical vibration analysis of nonlocal temperature-dependent FG nanobeams with various boundary conditions *Composites* B **78** 272–90

Ebrahimi F and Salari E 2015b Thermal buckling and free vibration analysis of size dependent Timoshenko FG nanobeams in thermal environments *Compos. Struct.* **128** 363–80

Eltaher M, Emam S A and Mahmoud F 2013 Static and stability analysis of nonlocal functionally graded nanobeams *Compos. Struct.* **96** 82–8

Eringen A C 1983 On differential equations of nonlocal elasticity and solutions of screw dislocation and surface waves *J. Appl. Phys.* **54** 4703–10

Eringen A C 2002 *Nonlocal Continuum Field Theories* (Berlin: Springer)

Fallah A and Aghdam M 2012 Thermo-mechanical buckling and nonlinear free vibration analysis of functionally graded beams on nonlinear elastic foundation *Composites* B **43** 1523–30
Fei P, Yeh P-H, Zhou J, Xu S, Gao Y, Song J, Gu Y, Huang Y and Wang Z L 2009 Piezoelectric potential gated field-effect transistor based on a free-standing ZnO wire *Nano Lett.* **9** 3435–9
Fu Y, Du H and Zhang S 2003 Functionally graded TiN/TiNi shape memory alloy films *Mater. Lett.* **57** 2995–9
Giunta G, Crisafulli D, Belouettar S and Carrera E 2011 Hierarchical theories for the free vibration analysis of functionally graded beams *Compos. Struct.* **94** 68–74
Giunta G, Crisafulli D, Belouettar S and Carrera E 2013 A thermo-mechanical analysis of functionally graded beams via hierarchical modelling *Compos. Struct.* **95** 676–90
He J H, Hsin C L, Liu J, Chen L J and Wang Z L 2007 Piezoelectric gated diode of a single ZnO nanowire *Adv. Mater.* **19** 781–4
Iijima S 1991 Helical microtubules of graphitic carbon *Nature* **354** 56–8
Ke L-L and Wang Y-S 2012 Thermoelectric-mechanical vibration of piezoelectric nanobeams based on the nonlocal theory *Smart Mater. Struct.* **21** 025018
Ke L-L, Wang Y-S and Wang Z-D 2012 Nonlinear vibration of the piezoelectric nanobeams based on the nonlocal theory *Compos. Struct.* **94** 2038–47
Kerman K, Lai B K and Ramanathan S 2012 Nanoscale compositionally graded thin-film electrolyte membranes for low-temperature solid oxide fuel cells *Adv. Energy Mater.* **2** 656–61
Kiani Y and Eslami M 2010 Thermal buckling analysis of functionally graded material beams *Int. J. Mech. Mater. Des.* **6** 229–38
Kiani Y and Eslami M 2013 An exact solution for thermal buckling of annular FGM plates on an elastic medium *Composites* B **45** 101–10
Kiani Y, Rezaei M, Taheri S and Eslami M 2011 Thermo-electrical buckling of piezoelectric functionally graded material Timoshenko beams *Int. J. Mech. Mater. Des.* **7** 185–97
Kim H S, Yang Y, Koh J T, Lee K K, Lee D J, Lee K M and Park S W 2009 Fabrication and characterization of functionally graded nano-micro porous titanium surface by anodizing *J. Biomed. Mater. Res.* B **88** 427–35
Komijani M, Kiani Y, Esfahani S and Eslami M 2013 Vibration of thermo-electrically post-buckled rectangular functionally graded piezoelectric beams *Compos. Struct.* **98** 143–52
Komijani M, Reddy J and Eslami M 2014 Nonlinear analysis of microstructure-dependent functionally graded piezoelectric material actuators *J. Mech. Phys. Solids* **63** 214–27
Lee Z, Ophus C, Fischer L, Nelson-Fitzpatrick N, Westra K, Evoy S, Radmilovic V, Dahmen U and Mitlin D 2006 Metallic NEMS components fabricated from nanocomposite Al–Mo films *Nanotechnology* **17** 3063
Lezgy-Nazargah M, Vidal P and Polit O 2013 An efficient finite element model for static and dynamic analyses of functionally graded piezoelectric beams *Compos. Struct.* **104** 71–84
Lü C, Lim C W and Chen W 2009 Size-dependent elastic behavior of FGM ultra-thin films based on generalized refined theory *Int. J. Solids Struct.* **46** 1176–85
Lun F, Zhang P, Gao F and Jia H 2006 Design and fabrication of micro-optomechanical vibration sensor *Microfabrication Technol.* **120** 61–4
Mashat D S, Carrera E, Zenkour A M, Al Khateeb S A and Filippi M 2014 Free vibration of FGM layered beams by various theories and finite elements *Composites* B **59** 269–78
Nateghi A and Salamat-talab M 2013 Thermal effect on size dependent behavior of functionally graded microbeams based on modified couple stress theory *Compos. Struct.* **96** 97–110
Nazemnezhad R and Hosseini-Hashemi S 2014 Nonlocal nonlinear free vibration of functionally graded nanobeams *Compos. Struct.* **110** 192–9
Niknam H and Aghdam M 2015 A semi analytical approach for large amplitude free vibration and buckling of nonlocal FG beams resting on elastic foundation *Compos. Struct.* **119** 452–62
Pradhan S and Mandal U 2013 Finite element analysis of CNTs based on nonlocal elasticity and Timoshenko beam theory including thermal effect *Physica* E **53** 223–32
Rahaeifard M, Kahrobaiyan M and Ahmadian M 2009 *Sensitivity Analysis of Atomic Force Microscope Cantilever made of Functionally Graded Materials* pp 539–44
Salehipour H, Shahidi A and Nahvi H 2015 Modified nonlocal elasticity theory for functionally graded materials *Int. J. Eng. Sci.* **90** 44–57
Shi Z and Chen Y 2004 Functionally graded piezoelectric cantilever beam under load *Arch. Appl. Mech.* **74** 237–47
Şimşek M and Yurtcu H 2013 Analytical solutions for bending and buckling of functionally graded nanobeams based on the nonlocal Timoshenko beam theory *Compos. Struct.* **97** 378–86
Tanner S M, Gray J, Rogers C, Bertness K and Sanford N 2007 High-Q GaN nanowire resonators and oscillators *Appl. Phys. Lett.* **91** 203117
Wan Q, Li Q, Chen Y, Wang T-H, He X, Li J and Lin C 2004 Fabrication and ethanol sensing characteristics of ZnO nanowire gas sensors *Appl. Phys. Lett.* **84** 3654–6
Wang Q 2002 On buckling of column structures with a pair of piezoelectric layers *Eng. Struct.* **24** 199–205
Wang Q 2005 Wave propagation in carbon nanotubes via nonlocal continuum mechanics *J. Appl. Phys.* **98** 124301
Wang Z L and Song J 2006 Piezoelectric nanogenerators based on zinc oxide nanowire arrays *Science* **312** 242–6
Witvrouw A and Mehta A 2005 The use of functionally graded poly-SiGe layers for MEMS applications *Funct. Graded Mater. VIII* **492** 255–60
Xiang H and Shi Z 2009 Static analysis for functionally graded piezoelectric actuators or sensors under a combined electro-thermal load *Eur. J. Mech.* A **28** 338–46
Yang J and Xiang H 2007 Thermo-electro-mechanical characteristics of functionally graded piezoelectric actuators *Smart Mater. Struct.* **16** 784
Zhang D-G 2013 Nonlinear bending analysis of FGM beams based on physical neutral surface and high order shear deformation theory *Compos. Struct.* **100** 121–6
Zhang Y, Liu G and Xie X 2005 Free transverse vibrations of double-walled carbon nanotubes using a theory of nonlocal elasticity *Phys. Rev.* B **71** 195404
Zhong Z and Yu T 2007 Electroelastic analysis of functionally graded piezoelectric material beams *J. Intell. Mater. Syst. Struct.* **19** 707–13
Zhu X and Meng Z 1995 Operational principle, fabrication and displacement characteristics of a functionally gradient piezoelectric ceramic actuator *Sensors Actuators* A **48** 169–76